



ELSEVIER

Contents lists available at ScienceDirect

Corrosion Science

journal homepage: www.elsevier.com/locate/corsci

Effect of irradiation on corrosion of 304 nuclear grade stainless steel in simulated PWR primary water

Ping Deng^{a,b}, Qunjia Peng^{a,c,*}, En-Hou Han^a, Wei Ke^a, Chen Sun^c, Zhijie Jiao^d^a Key Laboratory of Nuclear Materials and Safety Assessment, Institute of Metal Research, Chinese Academy of Sciences, Shenyang City, 110016, China^b School of Materials Science and Engineering, University of Science and Technology of China, Shenyang City, 110016, China^c State Power Investment Corporation Research Institute, Beijing, 102209, China^d Department of Nuclear Engineering and Radiological Sciences, University of Michigan, Ann Arbor, MI, 48109, USA

ARTICLE INFO

Keywords:

- A. Stainless steel
- B. TEM
- C. High temperature corrosion
- C. Intergranular corrosion

ABSTRACT

Effect of irradiation on corrosion of 304 nuclear grade stainless steel (304NG SS) in simulated primary water of pressurized water reactor was investigated. The investigation was conducted by comparing the microstructure of the oxide scale formed on the steel irradiated to different doses by proton. The results revealed that increasing irradiation dose promoted both the corrosion and intergranular corrosion of 304NG SS. This is attributed to the irradiation induced defects as well as the Cr depletion at the grain boundary in the steel.

1. Introduction

Irradiation-assisted stress corrosion cracking (IASCC) of austenitic stainless steel (SS) core components is one major concern for maintenance of nuclear power plants. The IASCC is a complex phenomenon as a result of the synergic effect of irradiation induced damage of the material, corrosion and stress [1–4]. Studies showed that increasing irradiation dose resulted in a higher degree of intergranular cracking [1,5–7]. The irradiation induced damage of the material includes the formation of dislocation loops, grain boundary segregation and hardening etc., which occur simultaneously at comparable rates and are all correlated with the increased cracking susceptibility [7–9]. Further, deformation of irradiated alloys led to dislocation channeling as a result of dislocation glide [4,10]. As such, deformation was localized into the channels in which dislocations were fed into the grain boundary region [11–13]. The change in deformation modes and the interaction of localized dislocation channels with the grain boundary promoted the IASCC [10–13].

To date, studies on the effect of irradiation on IASCC had mainly focused on the irradiation induced changes in microstructure and mechanical properties. The role of corrosion in IASCC, however, has not been paid sufficient attentions. According to the internal oxidation and slip-dissolution/oxidation mechanisms for stress corrosion cracking (SCC), oxide film rupture is the first step in the SCC process and thereby the corrosion behavior is crucial to SCC initiation [14,15]. In fact, a study reported that the irradiated SS that was resistant to intergranular cracking in 288 °C argon was susceptible to intergranular cracking in

high temperature water at the same temperature [11], suggesting an apparent effect of corrosion on IASCC. As such, attentions should also be paid on the corrosion behavior of irradiated alloys, in particular to the localized corrosion at grain boundary, in order to understand further the mechanism of IASCC.

In recent years, the effect of irradiation on corrosion in high temperature water has received increased attentions, while only a few studies have been reported. Jiao found no obvious acceleration of corrosion by post-irradiation in high temperature water [16], while Perrin et al. concluded oppositely [17,18]. The promotion of corrosion by in-situ proton irradiation was also reported by Wang et al. [19]. These studies suggest that the role of irradiation in corrosion has not been fully understood, particularly for the post-irradiation corrosion. Further, while studies by Perrin et al. concluded some effect of post-irradiation on corrosion of austenitic stainless steels in high temperature water [17,18], discussions on the effect of irradiation had been focused on the irradiation induced structural defects. The effect of the possible change in chemical composition by radiation-induced segregation (RIS) on corrosion, particularly to the localized corrosion at grain boundary, however, has received limited attentions. In addition, there is still a lack of detailed understanding of the quantitative dependence of the corrosion behavior of austenitic SS in high temperature water on irradiation doses.

This study focused on the effect of irradiation on corrosion of 304 nuclear grade (NG) SS in simulated primary water of pressurized water reactor (PWR). The objective is to correlate the irradiation dose to the overall corrosion, as well as the RIS to localized corrosion at the grain

* Corresponding author at: Key Laboratory of Nuclear Materials and Safety Assessment, Institute of Metal Research, Chinese Academy of Sciences, Shenyang City, 110016, China.
E-mail address: pengqunjia@yahoo.com (Q. Peng).

<http://dx.doi.org/10.1016/j.corsci.2017.08.010>

Received 29 April 2017; Received in revised form 29 July 2017; Accepted 13 August 2017
0010-938X/ © 2017 Elsevier Ltd. All rights reserved.

Table 1
Chemical composition (wt.%) of 304NG SS.

C	Mn	Si	S	P	Ni	Cr	Co	Fe
0.04	1.73	0.27	0.002	0.021	8.87	19.51	0.04	Bal.

boundary. Irradiation-induced structure of 304NG SS was characterized using transmission electron microscope (TEM). Corrosion behavior of the steel irradiated to various doses by proton was studied by exposure tests in simulated PWR primary water, followed by characterization of the oxide scale using scanning electron microscopy (SEM), X-ray photoelectron spectroscopy (XPS) and TEM.

2. Experimental

2.1. Material

The material used was solution annealed (SA) 304NG SS with a chemical composition listed in Table 1. Bar-type specimens with a dimension of 20 mm × 3 mm × 2 mm cut from the alloy were wet ground using SiC papers up to 3000 grit, and then polished by diamond pastes of 1.5- and 0.5- μm to obtain a mirror-like surface. After wet-polishing, the specimens were polished by 40-nm colloidal silica slurry for over 2 h to ensure the removal of residual strain prior to proton irradiation. Irradiations were conducted using the General Ionex Tandemron accelerator at the Ion Beam Laboratory of the University of Michigan. The specimens were irradiated with 2 MeV protons at 360 °C at a rate of approximately 6×10^{-6} displacement per atom (dpa) per second (dpa/s) to a dose of 0.5-, 1.5-, 3- and 5-dpa, respectively. The depth damage profile as calculated by the Stopping and Range of Ions in Materials 2008 (SRIM 2008) computer code is shown in Fig. 1 [20]. The damage profile is nearly uniform within the ~ 1 to $\sim 10 \mu\text{m}$ of the whole 20 μm -thick damaged layer, and shows an implantation peak at $\sim 18 \mu\text{m}$. Details about the proton irradiation process are available elsewhere [12,21].

2.2. TEM characterization of the irradiation induced defects and segregation

The SA, 0.5- and 3-dpa irradiated specimens were selected for characterization of the irradiation induced defect and grain boundary segregation by TEM. The specimens were electropolished in an electrolyte at 30 °C and 30 mA for 5 s to remove a damage layer of 3–4 μm thick from the irradiated surface. The electrolyte was prepared by 5 vol. % perchloric acid of 70 wt.% concentration and 95% vol.% ethanol of 99 wt.% concentration. Then the non-irradiated face of the specimen was exposed for wet grinding to reduce the thickness to be less than

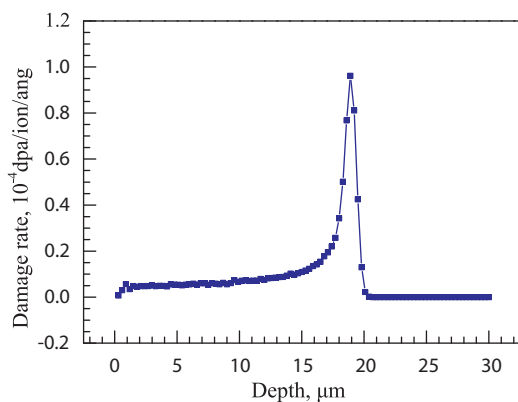


Fig. 1. Damage rate depth profile for 304NG SS irradiated with 2.0 MeV protons as calculated by SRIM 2008 computer code [20].

60 μm . TEM discs were then drilled out through the thinned specimens by a drill bit with a 3-mm inner diameter. These discs were thinned further from the non-irradiated side to electron transparency with a TenuPol-5 single-jet electropolisher, using the same electrolyte at $-20 \text{ }^\circ\text{C}$ and 30 V. Following the electro-thinning, microstructural characterization was conducted using a JEM-2100 TEM equipped with an energy dispersive X-ray spectroscopy (EDX). Spot analyses with a probe beam diameter of 1 nm were carried out to determine composition profiles across high-angle grain boundaries (HAGBs). Prior to the measurement, the grain boundary was aligned edge-on to the electron beam, which minimized the projected width of the grain boundary during sample tilting. In total more than 5 EDX line scans across the grain boundary were performed to calculate composition profiles for Cr and Ni. Faulted Frank dislocation loops were imaged by the rel-rod technique [22], and about 500 loops were imaged for each irradiation condition to obtain average loop diameters and number densities. Since the rel-rod image showed faulted loops from only one of the four sets of (1 1 1) planes, the number of faulted loops measured must be multiplied by four to get the total number of faulted loops [12,22]. The total number of faulted loops then divided by the volume involved in the picture gave the number density of the faulted loops. Thickness of the local area where the dislocation loops were imaged was determined from the electron energy-loss spectrum (EELS) by measuring the ratio of the zero loss peak intensity to that of the total spectrum [23].

2.3. Exposure test

After irradiation, the specimens were polished again by 40-nm colloidal silica slurry for half an hour to get fresh surfaces, which removed the surface with a thickness of 1–2 μm and could ensure that the specimen surfaces following different doses of irradiation were consistent. Then the exposure testing was conducted at 320 °C in simulate PWR primary water in a 3-L autoclave made of 316 SS, which is equipped with a refreshed water loop. The water contained 1200 mg/L of B as H_3BO_3 and 2.3 mg/L of Li as $\text{LiOH}\cdot\text{H}_2\text{O}$, with a dissolved hydrogen (DH) concentration of 2.6 mg/L at the inlet. The DH was achieved by applying a hydrogen overpressure of 0.08 MPa in the water tank of the loop, following removal of air in the water by bubbling hydrogen. To study the effect of irradiation dose on corrosion, in total four doses at 0.5, 1.5, 3 and 5 dpa as well as the SA specimens with no irradiation were employed for the exposure tests with a fixed exposure period of 500 h. After the exposure, the specimens were removed from the autoclave for characterization of the oxide scale.

2.4. Analysis of the oxide scale

Following the exposure tests, characterization of the oxide scales formed on the SA, 0.5-, 1.5-, 3- and 5-dpa specimens were performed to clarify the corrosion behavior. The surface morphology of the oxide scale was examined by a FEI XL30 Field Emission Gun SEM operating at 15 kV. The depth profile of the oxide scale was analyzed with an ESCALAB 250 XPS system. A selected area of 2-mm diameter was sequentially sputtered using a 2 keV Ar ion beam at a rate of 0.1 nm/s referred to Ta_2O_5 layer. More details about the XPS analysis were presented elsewhere [24]. Since XPS sputtering is a homogeneous process, the depth profiles consist of average element concentrations, which depend on the local structure of the oxide scale. Therefore, the recorded depth profiles were only used to estimate the thickness of the oxide scale as a function of irradiation dose. The accurate depth profile on the cross-section of the oxide scale was analyzed using a JEM-2100 TEM operating at 200 kV. The TEM is equipped with scanning capabilities for producing chemical contrast images and the EDX device for the composition analysis. Both point- and area-scans were used to analyze the chemical composition of the oxide scale. High-resolution TEM images were captured by a Gatan 4k charge coupled device camera and analyzed using Fast Fourier Transform (FFT) technique to

Download English Version:

<https://daneshyari.com/en/article/5439809>

Download Persian Version:

<https://daneshyari.com/article/5439809>

[Daneshyari.com](https://daneshyari.com)